Chapter 6

Effective diffusivities in laterally heated double-diffusive systems

The effective vertical diffusivity for salt is estimated for laterally heated double-diffusive layered structures. First, the vertical interfacial salt fluxes are calculated using data retrieved from five different numerical simulations. The salt fluxes are shown to be consistent with the flux law for a diffusive interface, derived from laboratory experiments. The fluxes appear to be independent on the buoyancy (stability) ratio over the interface for the range considered and for a typical Rayleigh number (based on the horizontal temperature difference and vertical layer scale η) of $Ra_\eta = O(10^5)$. The effective vertical salt diffusivity K_S is almost five times larger than the molecular salt diffusivity κ_S but is much smaller than the values available for oceanic layered structures ($Ra_\eta = O(10^9)$). An extrapolation towards $Ra_\eta = O(10^9)$ yields a value of the same order as determined from measurements, namely $K_S = O(10^{-7})\ m^2 s^{-1}$, indicating that the vertical effective salt diffusivities are of the same order for both laterally and vertically cooled double-diffusive structures.

6.1 Introduction

The previous chapters have shown that the lateral heating or cooling of a stable salinity gradient can lead to the formation of a layered structure consisting of horizontal convective layers separated by thin diffusive interfaces. In these interfaces the vertical velocity is (almost) zero, leaving only vertical diffusion as a possible transport mechanism. However, the convection has strongly modified the salinity gradient in the interface, resulting in an increased vertical salt flux. In this

Case	Ra_η	R
1	$5\ 10^4$	5
2	$2\ 10^5$	5
3	$5\ 10^4$	2.5
4	$1\ 10^6$	2.5
5	$5\ 10^4$	10

Table 6.1: *The parameters distinguishing the five simulations.*

chapter, an estimate of the vertical effective salt diffusivity will be determined.

If a stable salt gradient is heated from below, a layered structure is formed which is very similar (although with a different layer scaling [*Turner*, 1973]) to the laterally heated cases, i.e. well-mixed convective layers are formed separated by diffusive interfaces in which steep temperature and salt gradients are present. Flux laws have been derived for the vertical heat and salt fluxes across these interfaces [*Huppert*, 1971]. Effective vertical diffusivities for heat and salt have been determined for oceanographic double-diffusive layered structures [*Kelley*, 1984] using these flux laws because these structures were assumed to be generated by vertical thermal forcing. Main goal was to express the fluxes in terms of overall temperature and salinity differences, in order to parametrize the large-scale transports induced by the structures. In our laterally heated model simulations, the vertical salt distribution is akin to the distribution in vertically heated or cooled systems, and this gives rise to the question whether the flux law for the vertical salt flux also applies to our results.

High-resolution simulations like those in Chapter 3 are necessary to determine the interfacial fluxes accurately. Due to the absence of a thermal background stratification in the simulations (generally, no-flux conditions for temperature at the lower and upper boundaries apply and an initial thermal gradient is absent too) it is not possible to derive a vertical effective thermal diffusivity. Therefore only the effective vertical salt diffusivity K_S will be determined.

In this chapter an estimate of the vertical salt flux will be derived from five different numerical simulations. The applicability of the flux law is investigated. Next, K_S is calculated and extrapolated towards higher Rayleigh numbers relevant for oceanographic conditions and compared to the results of *Kelley* [1984]. The consequence for the generation mechanism of oceanographic double-diffusive structures is discussed.

Case	R_ρ	δT	δS	$-\partial S/\partial z$	$10^2 \Phi_S$	$10^2 F_S$
1	7.70	0.136	0.209	2.986	3.0	4.5
1	10.05	0.087	0.175	2.692	2.7	3.6
1	11.45	0.075	0.172	3.127	3.1	3.5
1	11.55	0.081	0.187	3.400	3.4	3.9
2	4.70	0.155	0.146	3.244	3.2	4.4
2	6.16	0.129	0.159	3.975	3.9	5.0
2	7.45	0.100	0.149	3.725	3.7	4.6
2	8.80	0.124	0.218	5.450	5.4	7.6
3	4.28	0.174	0.297	4.569	4.5	2.9
3	4.52	0.180	0.326	4.075	4.0	3.2
4	2.10	0.233	0.197	2.627	2.6	4.5
4	3.22	0.173	0.223	4.660	4.6	5.3
4	3.55	0.169	0.240	4.800	4.8	5.8
5	11.20	0.118	0.132	2.933	2.9	6.2
5	16.20	0.106	0.172	3.440	3.4	8.8

Table 6.2: *The local values of the dimensionless variables used for the calculation of the vertical dimensionless salt fluxes across the interfaces. Also shown are the resulting values of Φ_S (6.1) and F_S (6.3).*

6.2 The salt fluxes over the diffusive interfaces

For the calculation of the salt fluxes over the diffusive interfaces, the results of five different simulations were used. The parameters of these simulations are given in Table 6.1 (for definitions of these parameters, see Chapter 3). Cases $1-3$ correspond to the results of the simulations in Chapter 3 taken at $t = 0.1$, but for cases $4-5$ new simulations were performed with either larger Ra_η (case 4) or larger R (case 5). The other parameters retained the same value, i.e. $Pr = 7$, $Le = 101$ and $A = 1$. For these simulations the same integration method and gridsize were used as for cases $1-3$, i.e. explicit time integration on a 201*201 grid. The layered structures visible at $t = 0.1$ for the five cases are shown in Fig. 6.1 in the form of salinity plots. For all cases the layer scale $\eta = \alpha \Delta T / \beta \Phi_0$ (the heigth a fluid parcel containing a heat surplus ΔT would rise in a linear salinity gradient with strength $\Phi_0 = -\partial S/\partial z$ until density equalisation occurs) appears to be valid. To calculate the jumps in temperature and salinity across the diffusive interfaces, vertical sections of the temperature and salinity were taken at the centre of the cavity and are

shown in Fig. 6.2. Only those interfaces were regarded over which the temperature gradients were well-developed. The resulting jumps and the corresponding salt gradients are presented in the left part of Table 6.2. Here δT and δS are the jumps in temperature and salinity across the interfaces, and R_ρ is the (local) stability ratio defined as $R_\rho = \beta \delta S^* / \alpha \delta T^* = R \delta S / \delta T$ (stars denoting dimensional quantities).

The dimensionless vertical salt flux Φ_S across each interface can be calculated from:

$$\Phi_S = -Le^{-1} \frac{\partial S}{\partial z} \tag{6.1}$$

and is tabulated in Table 6.2. An estimate of the vertical salt flux is then obtained by averaging the column values of Φ_S in Table 6.2:

$$\Phi_S = 3.7 \; 10^{-2}. \tag{6.2}$$

A comparison with the purely diffusive flux, equal to $Le^{-1} = 1 \; 10^{-2}$, shows that convection has lead to a fourfold increase of the vertical salt flux.

At this point we check whether the vertical salt flux satisfies the flux law for diffusive interfaces. In Appendix C a flux law for the vertical salt flux is derived for a double-diffusive system where the vertical salinity distribution has a characteristic "step"-structure, i.e. salt is well-mixed in the convective layers, whereas strong salinity gradients exist within the diffusive interfaces. In our laterally heated cases the vertical salinity distribution corresponds has this step-like structure, in contrast with the vertical temperature distribution. Therefore, according to Appendix C, expression (C.8), we use the following expression for the dimensionless vertical salt flux F_S:

$$F_S = c_S \, (Ra_\eta R^4)^{1/3} \, (-\delta S)^{4/3}. \tag{6.3}$$

As a test of the validity of flux law (6.3) the quantity $(F_S / (Ra_\eta R^4)^{1/3})^{3/4}$ is plotted against δS in Fig. 6.3. Fig. 6.3 clearly reveals a linear relationship, which indicates that c_S is a constant. Due to scatter a range of slopes is possible; based on extremal values we derive the following range of values for c_S:

$$\text{range } c_S \in [1.15 \; 10^{-3}, \; 4.29 \; 10^{-3}].$$

The minimum of this range provides a good value for c_S;

$$c_S = 1.15 \; 10^{-3}. \tag{6.4}$$

Using this value, F_S is calculated for each interface and presented in Table 6.2. Averaging these values gives an estimate of the salt flux as calculated with the flux law (6.3):

$$F_S = 4.9 \; 10^{-2}. \tag{6.5}$$
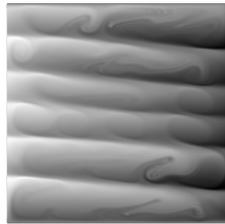
Case 1:
$Ra_\eta = 5\ 10^4$,
$R = 5$
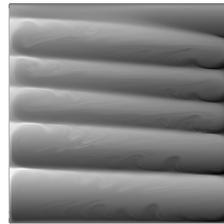
Case 2:
$Ra_\eta = 2\ 10^5$,
$R = 5$
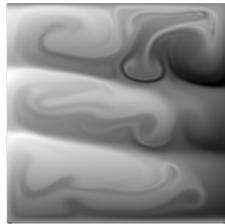
Case 3:
$Ra_\eta = 5\ 10^4$,
$R = 2.5$
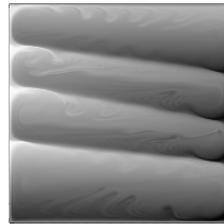
Case 4:
$Ra_\eta = 1\ 10^6$,
$R = 2.5$
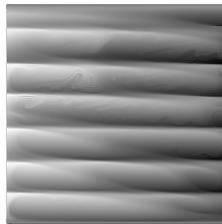
Case 5:
$Ra_\eta = 5\ 10^4$,
$R = 10$

Figure 6.1: *Grey-scale plots of the five cases; shown is the salt distribution minus the initial linear stratification.*
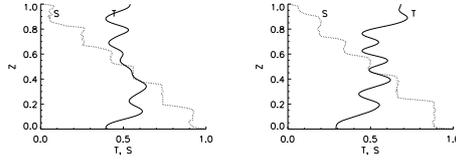
Case 1:
$Ra_\eta = 5 \ 10^4,$
$R = 5$

Case 2:
$Ra_\eta = 2 \ 10^5,$
$R = 5$
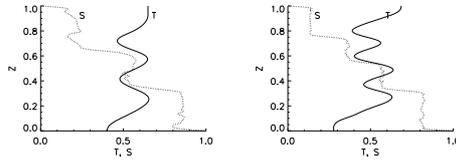
Case 3:
$Ra_\eta = 5 \ 10^4,$
$R = 2.5$

Case 4:
$Ra_\eta = 1 \ 10^6,$
$R = 2.5$
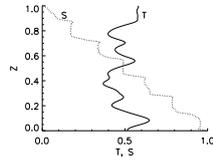
Case 5:
$Ra_\eta = 5 \ 10^4,$
$R = 10$

Figure 6.2: *Vertical sections of T and S through the centre of the container for each case.*

The estimates (6.2) and (6.5) are of the same order, which shows that the flux law can be applied with succes in laterally heated double-diffusive systems.
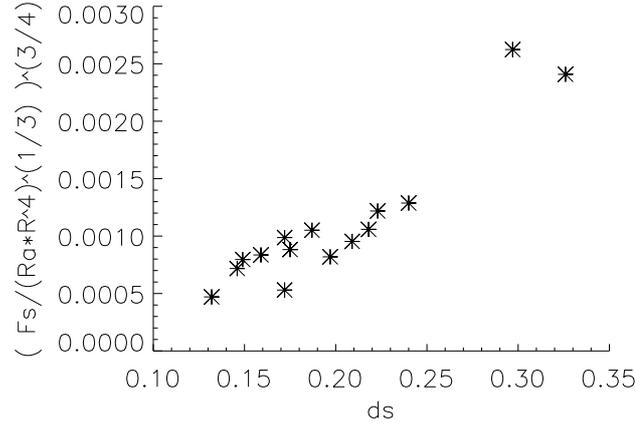
Figure 6.3: *Plot of* $(F_S/(Ra_\eta R^4)^{1/3})^{3/4}$ *as a function of* δS.

The effective dimensionless vertical salt diffusivity K_S can be defined as the ratio of the estimated vertical salt flux (6.5) and the dimensionless vertical background salt gradient. Since the latter equals one, we have the following estimate:

$$K_S = 4.9 \, 10^{-2}. \tag{6.6}$$

Finally, the dimensional diffusivity K_S^* results from the application of the scales H and H^2/κ_T for length and time respectively:

$$
\begin{aligned}
K_S^* &= \kappa_T \, K_S & (\kappa_T = 1.4 \, 10^{-7} \, \text{m}^2\text{s}^{-1}) \\
&= 6.9 \, 10^{-9} \, \text{m}^2\text{s}^{-1} \, .
\end{aligned}
\tag{6.7}
$$

6.3 Discussion

The vertical salt flux in a laterally heated double-diffusive system has been shown to satisfy the flux law (6.3) for a diffusive interface. This is to be expected since, in our simulations, the vertical salt distribution is such that salt is well mixed in the convective layers, while steep salt gradients

exist in the interfaces; a situation which applies also to layered double-diffusive structures that are thermally forced from below. For the range of Ra_η considered, the salt flux F_S appears to be independent of the stability ratio R_ρ, in contrast with oceanographic conditions at much larger Ra_η [*Kelley*, 1984], where the interfaces become less stable for small values of R_ρ [*Huppert*, 1971], resulting in an increased salt flux . The stability of the interfaces in our simulations is clear when the salinity perturbation plots in Fig. 6.1 are considered; the interfaces between the layers are clear and convection in the layers between the interfaces does not appear to destroy them. The estimate of K_S^* that has been determined for the simulations ($K_S^* = 6.9\ 10^{-9}$ m^{2}s^{-1}) is about five times larger than the molecular salt diffusivity ($\kappa_S = 1.4\ 10^{-9}$ m^{2}s^{-1}). This value is probably not very accurate since a range of values of c_S is possible. This is caused by scatter in Fig. 6.3 which may be attributed to the fact that some layers are not fully developed (for example in case 3, which becomes clear from Fig. 6.1c). Yet, the value chosen is of the same order as the salt diffusivity which has been calculated directly from the local salt gradients over the interfaces.

It is of interest to know whether the determined value of K_S^* is relevant in an oceanographical context. *Kelley* [1984] estimated the values of both thermal and saline diffusivity coefficients from oceanographic measurements of double-diffusive layered structures. He assumed that these layers were formed as a result of vertical cooling. Therefore we have to extrapolate K_S^*, estimated for $Ra_\eta = O(10^5)$, to values representative of oceanographic conditions as measured by *Kelley* [1984] ($Ra_\eta = O(10^9)$). Firstly, we show that the saline diffusivity is a function of Ra_η only. We start with expressing (6.3) in terms of the layer thickness scale η which has been shown both experimentally and numerically in the previous chapters to be valid for a large range of Rayleigh number. Assuming that the steps over the diffusive interfaces are of the same strength, the relation $\eta = H/R$ implies:

$$\delta S = O(R^{-1}). \tag{6.8}$$

Substituting this expression into (6.3), we arrive at:

$$F_S = c_S\ Ra_\eta^{1/3}, \tag{6.9}$$

which indeed shows that F_S - and therefore F_S^* and K_S^* - depends on Ra_η only.

An increase of Ra_η with a factor $O(10^4)$ results in $K_S^* = O(1.4\ 10^{-7}$ m^{2}s$^{-1})$. This value is certainly in the range of K_S^* as calculated by *Kelley* [1984] and depicted in his Figure 2. This result indicates that the vertical salt fluxes for vertically and laterally forced systems are the same. Still, more simulations are necessary, especially for $Ra_\eta > 10^5$, to determine accurate values for the effective salt diffusivity.

References

Huppert, H. E., On the stability of a series of double-diffusive layers, *Deep-Sea Res.*, 18, 1005-1021 (1971).

Kelley, D., Effective diffusivities within oceanic thermohaline staircases, *J. Geophys. Res.*, 89, 10,484-10,488 (1984).

Turner, J. S., *Buoyancy effects in fluids*, Cambridge (1973).